

# Salt Dependence of the Formation and Stability of the Signaling State in G Protein-Coupled Receptors: Evidence for the Involvement of the Hofmeister Effect<sup>†</sup>

Reiner Vogel,<sup>\*,‡</sup> Gui-Bao Fan,<sup>§</sup> Mordechai Sheves,<sup>§</sup> and Friedrich Siebert<sup>‡</sup>

Sektion Biophysik, Institut für Molekulare Medizin und Zellforschung, Albert-Ludwig-Universität Freiburg, Albertstrasse 23, D-79104 Freiburg, Germany, and Department of Organic Chemistry, Weizmann Institute of Science, Rehovot 76100, Israel

Received August 8, 2000; Revised Manuscript Received October 16, 2000

**ABSTRACT:** We studied the salt dependence of both the stability and the equilibrium of the late photoproducts metarhodopsin I (MI) and II (MII) of the artificial visual pigment 9-demethyl rhodopsin (9dm-Rho). In the photoproducts of 9dm-Rho, *all-trans*-9-demethyl retinal acts only as a partial agonist, enabling us to study the photoproduct equilibrium of the pigment both in membranes and in detergent micelles. Chloride, bromide, and phosphate salts shift this equilibrium from the inactive MI to the active MII receptor conformation both in native membranes and even more with purified pigment in detergent micelles. In the presence of these salts, the induced MII state seems to be structurally intact, as judged by Fourier transform infrared (FTIR) and UV–vis spectroscopy. In the long term, however, we observe an increased instability of the photoproducts and a change in the decay pathways. Both MII enhancement and destabilization are particularly pronounced with the strong chaotropic salts KI and KSCN. The results fit into the framework of the Hofmeister effect and are assigned to an increased solvation of the peptide moiety of the solvent-exposed domains, their resulting partial disordering favoring MII over MI. In this picture, increased solvation also affects helix–helix interactions, thereby leading to a structural instability of the protein in the long term. The reported influences of salts on conformation and stability of this membrane protein are likely to be general and may therefore also apply to other transmembrane proteins and particularly to other G protein-coupled receptors.

The membrane protein rhodopsin is the visual pigment responsible for dim light vision and serves as a prototype in the family of G protein-coupled receptors (GPCRs)<sup>1</sup> (1–5). In the dark, its covalently bound chromophore 11-*cis*-retinal acts as an inverse agonist and keeps the protein in an inactive dark conformation. Upon photon absorption, the chromophore isomerizes to an *all-trans* geometry and acts as a full agonist, driving the photoproduct equilibrium between the active conformation (metarhodopsin II, MII) and its still inactive precursor MI almost entirely to the MII side under physiological conditions. This equilibrium can be shifted more to the MI side by increasing pH (6), decreasing temperature (6), increasing pressure (7), or increasing rigidity of the embedding matrix (8). It was recently shown that it is

also influenced by salts (9, 10), which shift the equilibrium to the MII side, the reason for this, however, not being clear. In another study, a salt-induced shift to the MI side was observed at low salt concentrations and shown to be due to a salt dependence of the local surface pH at the protein–solvent interface in comparison to the bulk pH (11).

Scanning through the literature, we found other examples of salt dependent effects on conformational and/or functional states of a variety of proteins. Many of the reported effects on protein stability and conformation can be correlated with the so-called Hofmeister series of neutral salts after Franz Hofmeister, who was the first to describe this phenomenology in 1888 (12) [for recent reviews cf. refs 13 and 14]. First only empirically and later also on a molecular level, salts were distinguished into chaotropic salts, which destabilize and denature proteins, and cosmotropes, which are stabilizers and may induce crystallization of proteins.

In general, the Hofmeister effect is based on salt-specific changes of the properties of the aqueous phase–protein interface via two opposing mechanisms: (i) by decreasing the solvation (salting out) of hydrophobic groups and (ii) by increasing the solvation (salting in) of the polar peptide backbone (15). The first effect is due to a salt-dependent increase of the water surface tension, which in turn also increases the free energy required to form a cavity in the aqueous phase for accommodation of a rather hydrophobic residue. The order of ions in their ability to increase the surface tension of water was found to follow  $\text{SCN}^- < \text{I}^- < \text{Br}^- < \text{Cl}^- < \text{F}^- < \text{SO}_4^{2-}$  and  $\text{Li}^+ < \text{Na}^+ < \text{K}^+ < \text{Mg}^{2+} <$

<sup>†</sup> We gratefully acknowledge financial support by grants from the Deutsche Forschungsgemeinschaft to R.V. (Grant VO 811/1-1) and to F.S. (Grant SI 278/16-2,3), by Fonds der Chemischen Industrie (to F.S.), by a grant from the A.N.M. fund for the promotion of Science, Culture, and Arts in Israel (to M.S.), and by the US-Israel Binational Science Foundation (to M.S.).

\* To whom correspondence should be addressed. Reiner Vogel, Sektion Biophysik, Institut für Molekulare Medizin und Zellforschung, Albert-Ludwig-Universität Freiburg, Albertstr. 23, D-79104 Freiburg, Germany, Telephone: +49 761 203 5391, Fax: +49 761 203 5016, E-mail: vogelr@uni-freiburg.de.

<sup>‡</sup> Institut für Molekulare Medizin und Zellforschung.

<sup>§</sup> Weizmann Institute of Science.

<sup>1</sup> Abbreviations: 9dm-Rho, 9-demethyl rhodopsin;  $\phi$ : photoconversion factor; DM, *n*-dodecyl- $\beta$ -D-maltoside; FTIR, Fourier transform infrared; GPCR, G-protein coupled receptor; MI, MII, metarhodopsin I and II; MII<sub>380</sub>, MII<sub>470</sub>, MII subspecies with a deprotonated and protonated retinal Schiff base, respectively; MES, 2-[*N*-morpholino]-ethanesulfonic acid; MOPS, 3-[*N*-morpholino]propanesulfonic acid.

$\text{Ca}^{2+}$  in agreement with their salting-out properties (15–17). The second mechanism, the salting-in of the peptide group, is less well understood (15). It could be shown that the destabilizing action of chaotropic salts involves an increased solvation of the peptide moiety of the protein backbone and that the ability of ions to salt in model peptides (oligo-Gly) increases with  $\text{SO}_4^{2-} < \text{F}^- < \text{Cl}^- < \text{Br}^- < \text{I}^- < \text{SCN}^-$  and  $\text{Li}^+ < \text{Na}^+ < \text{K}^+ < \text{Ca}^{2+}$  (18). Salts can affect the free energy of the solution process  $(\Delta G^\circ)_{\text{solution}} = (\Delta G^\circ)_{\text{cavitation}} + (\Delta G^\circ)_{\text{protein solvation}}$  by acting on either of the two energy terms. As the salts under consideration are all increasing the water surface tension and therefore increasing the first term representing the energy required for forming a cavity in the solvent, a salting-in process must involve a lowering of the second term, the free energy of the protein–solvent interaction itself (19). Increased solvation and therefore a partial unfolding of a protein may then be only the first steps on the way to its denaturation (15). In summary, salts may both stabilize proteins by salting out hydrophobic groups and simultaneously destabilize them by salting in the peptide group, both to a different extent. The property of a certain salt to act as a stabilizer or a destabilizer on a certain protein is therefore the result of a balance between these two opposing effects (15), and the terminology chaotrope or cosmotrope does not describe an invariant property of a salt alone, but must always include the protein and sometimes even the salt concentration under consideration.

Much of what is known experimentally about the effects of salts on the stability of proteins comes from soluble proteins. The salt dependence of the stability of bovine serum albumin and  $\beta$ -lactoglobulin, for example, shows distinct differences, presumably reflecting the differing contents of  $\alpha$ -helical and  $\beta$ -sheet secondary structure and underlining the specificity of both salt and protein for the Hofmeister effect (20, 21). Other studies report on salt-dependent conformational transitions, activity changes, and stabilization/destabilization of a broad variety of other proteins (22–29).

To examine the effect of salts on the  $\text{MI} \rightleftharpoons \text{MII}$  equilibrium of rhodopsin in detail both in native membranes and with purified pigment in detergent micelles, we had to overcome the strong favoring of MII over a broad temperature range. Therefore, we used a model system, in which the native retinal chromophore was replaced by the analogue 9-demethyl retinal. Previous studies on photoreceptor cells regenerated with this analogue have shown that both signal transduction and deactivation in these cells is considerably impaired (30, 31). Other studies clearly showed that the 9-methyl group of retinal is essential for formation of the active state of rhodopsin (32, 33) and that substitution of this group by a hydrogen renders the chromophore, in its all-trans form, from an agonist to an only partial agonist (34, 35). With this model pigment 9-demethyl rhodopsin (9dm-Rho), we show that its  $\text{MI} \rightleftharpoons \text{MII}$  equilibrium can be shifted considerably by salts to the MII side, both for the pigments in membranes and in detergent micelles, and that this effect does not saturate at higher salt concentrations. In addition to the shift in the photoproduct equilibrium, there is also a salt-dependent increased structural instability of the photoproducts in the long term. The anion specificity is striking, with  $\text{SCN}^-$  and  $\text{I}^-$  being by far both the strongest MII enhancers and the strongest destabilizers in membranes and in detergent micelles. Chloride, bromide, sulfate, and phos-

phate ( $\text{H}_2\text{PO}_4^-$ ), in increasing order, are intermediate in both respects (but still in the same direction). We also observe a cation dependence with  $\text{K}^+ \approx \text{Na}^+ \leq \text{Mg}^{2+} < \text{Ca}^{2+}$  in order of increasing chaotropy.

All examined salts exhibit MII enhancement and destabilizing properties. We therefore suggest that the mechanism of action of Hofmeister salts on the 9dm-Rho photoproducts must be seen primarily in the interaction of the salts with the peptide backbone of solvent-exposed domains by a sequential mechanism: The observed equilibrium shift to MII is then due to the favoring of a partially unfolded form of the (presumably cytoplasmic) domain in MII over a more ordered form in MI as a first step. From FTIR and UV–vis spectroscopy we conclude that photoproducts themselves remain structurally intact during this process. The salt-induced overall structural instability of the photoproducts as a second step is observed on longer time scales. It obviously involves a change in the whole protein's helix packing structure putatively due to a salt-induced weakening of helix–helix association by increasing solvation.

It is widely accepted that all members of the GPCR family of membrane receptor proteins share a common architecture (1, 5). Recent experimental work suggests that the major structural changes defining the activation of rhodopsin are also shared by other GPCRs (3, 36, 37). Very likely, salts act similarly on equilibria between active and inactive receptor states of GPCRs in general. Understanding their mode of action on these equilibria is therefore desirable and may lead to a better understanding of the processes involved in receptor activation and possibly also give insight into more general aspects of the stability of membrane proteins.

## EXPERIMENTAL PROCEDURES

**Preparation of the Pigment.** Bovine rhodopsin in washed rod outer segment disk membranes was prepared essentially as described previously from cattle retinae (38). 9dm-Rho in membranes was prepared from rhodopsin by removal of the covalently bound retinal chromophore and subsequent regeneration of the opsin with synthetic 11-cis 9dm-retinal (34, 39). Purified pigment was prepared in dodecyl maltoside (DM; Anatrace, OH, and Biomol, Germany) on a concanavalin A Sepharose column (Pharmacia Biotech, Sweden) (40). Pigments in membranes and in detergent were stored in distilled water at  $-20^\circ\text{C}$ . All manipulations involving rhodopsin or 9dm-Rho were performed under dim red light.

**Determination of MII Content.** MII formation was determined by two different methods, for pigment in membranes by FTIR spectroscopy and for pigment in detergent mainly with UV–vis spectroscopy.

**UV–Visible Spectroscopy.** UV–visible absorption spectroscopy was performed with a Perkin-Elmer Lambda 17 UV–vis spectrophotometer equipped with a thermostated cuvette holder (stability  $\pm 0.2^\circ\text{C}$ ). Spectra from pigment solutions in 20 mM buffer and 0.1% DM were measured in microcuvettes with a 10-mm path length. MES and MOPS buffers were found to be inert with respect to the  $\text{MI} \rightleftharpoons \text{MII}$  equilibrium, and samples declared “w/o salt” also contained 20 mM of one of these buffers. The spectra were background and offset corrected (at 650 nm). For light-induced difference spectra, the samples were illuminated for 30 s by a 150 W slide projector through a GG475 long-pass filter (Schott,

Germany) connected to a fiber optic. These conditions were exactly reproduced in all experiments and were found to be sufficient for establishing a photostationary state. Immediately after illumination, successive spectra were recorded with an acquisition time of 90 s each. By comparison of these successive spectra, we addressed a possibly slow temporal evolution of the MI  $\rightleftharpoons$  MII equilibrium over the time required for data acquisition. In all experiments, however, the first spectrum recorded after sample illumination already corresponded to a steady state of the photoproduct equilibrium. Under some conditions, as for example, higher temperatures or with strong chaotropic salts, there were significant spectral changes already within the first few minutes after illumination, which were, however, due to MII decay and which will be stated in the text in these cases. Before evaluation of the UV-vis data, we also checked routinely, whether the salt-induced spectral changes reflect rather a shift of the photoproduct equilibrium or a change of the spectral properties of the photoproducts. Unless stated otherwise, the absorbance maxima were at the same position as observed under low to isotonic salt conditions (this applies also to the dark state).

For a determination of the MII<sub>380</sub> yield, the absorbance change at 380 nm,  $\Delta A_{380}$ , was measured and normalized by the absorbance of the dark pigment at  $\lambda_{\max}$  464 nm before illumination ( $A_{464 \text{ dark}}$ ). Because of photoregeneration of the dark state [i.e., a light-induced re-isomerization of *all-trans*-retinal in the photoproducts to the 11-*cis* geometry of the dark state, as shown previously (34)], there is never a full conversion of the dark state into the photoproduct state under photostationary conditions [for simplicity, we will use the term photoproduct only for MI and MII and not for the photoregenerated dark state]. As the absorption peaks of the dark state MI and MII<sub>470</sub> almost coincide ( $\lambda_{\max}$  470 nm), we determined the amount of photoregenerated dark pigment by addition of hydroxylamine to the samples after illumination and subsequent warming to 25 °C in the dark. As hydroxylamine reacts with the photoproducts of 9dm-Rho forming opsin and retinal oxime ( $\lambda_{\max}$  357 nm), but not with the dark state, this method allows one to discriminate between the photoproducts and the photoregenerated dark state. We found that the degree of photoconversion  $\varphi$  (i.e., the amount of photoproduct under photostationary conditions normalized by the total amount of pigment) increases with the amount of MII<sub>380</sub> being formed, as this species cannot be directly photoconverted to the ground state by light with  $\lambda > 475$  nm but only via the photoproduct equilibrium.  $\varphi$  was empirically found to depend linearly on the amount of MII<sub>380</sub> formed according to the relation  $\varphi = \alpha + \beta \cdot A_{380}/A_{464 \text{ dark}}$  (data not shown) with temperature-dependent coefficients  $\alpha$  and  $\beta$ . By least-squares fits, we obtained for  $\alpha$  and  $\beta$  the values 0.47 and 1.16 at 1 °C, 0.44 and 0.87 at 10 °C, and 0.44 and 0.70 at 15 °C, respectively.  $\alpha$  can be interpreted as the photoconversion factor for a pure MI state and is quite temperature-independent, while  $\beta$  reflects the composition of the 470 nm photoproduct (consisting of MI and MII<sub>470</sub>). Its negative correlation with temperature presumably reflects the increase of the MII<sub>380</sub>/MII<sub>470</sub> ratio with temperature in the presence of salts (see Results and Discussion). To obtain the contribution of MII<sub>380</sub> to the photoproduct [i.e., MII<sub>380</sub>/(MI + MII)], the normalized MII<sub>380</sub> yield was corrected by division by  $\varphi$ .

**FTIR Spectroscopy.** FTIR spectroscopy was performed with a Bruker IFS 28 FTIR spectrometer, equipped with a liquid nitrogen-cooled HgCdTe detector and a dry air purged measuring chamber. The sample holder was thermostated by a circulating water bath with a reproducibility and stability of the temperature of  $\pm 0.1$  °C. As a common problem with IR spectroscopy, the absolute temperature cannot be directly measured in the sample but only at the sample holder. Because of the long equilibration time prior to the measurement, the temperature difference between sample and sample holder should not vary between measurements and is estimated to be less than 0.5 °C. Difference spectra were calculated from each 512 scans recorded at a 4 cm<sup>-1</sup> resolution before and after illumination. Samples were illuminated for 30 s with light with  $\lambda > 420$  nm and subsequently left in the dark for an additional 30 s to reduce an illumination-induced slight sample warming. Acquisition time for 512 scans was 60 s.

Spectra were taken from sandwich samples, prepared on specially designed CaF<sub>2</sub> windows by drying 0.5–1 nmol of pigment on a round spot of 7-mm diameter, separated from the 4  $\mu$ m higher rim of the window by a 1-mm wide depression. The dried samples were hydrated by approximately 0.7  $\mu$ L of buffer containing the respective salt in final concentration and 100 mM MES (also the samples “w/o salt”) adjusted to the desired pH and sealed by placing a second, plane window onto the first window with its higher rim serving as a spacer. Amount of pigment and buffer were not varied within the single series of experiments.

The MII contribution to the photoproducts was determined essentially as described previously (34). As marker bands, we used characteristic MII differential bands in the range of the stretching frequencies of protonated carboxyl groups assigned to Asp<sup>83</sup> and Glu<sup>122</sup> (41) (indicated in Figure 1, panel A). We examined the amplitude of the -1768/+1750 cm<sup>-1</sup> and the +1750/-1726 cm<sup>-1</sup> difference bands for detergent samples and the -1767/+1750 cm<sup>-1</sup> and +1710/-1695 cm<sup>-1</sup> difference bands for membrane samples. We estimate the error inherent in this method to be around 10% (absolute).

## RESULTS AND DISCUSSION

**Properties of the 9dm-Rho Photoproducts.** In this section, we will shortly summarize previously published results on rhodopsin and 9dm-Rho. In contrast to *all-trans*-retinal in the photoproducts of native rhodopsin, the artificial chromophore *all-trans* 9dm-retinal is acting only as a partial agonist on the photoproduct equilibrium of 9dm-Rho. The MI  $\rightleftharpoons$  MII equilibrium is therefore shifted to the MI side in 9dm-Rho ( $\lambda_{\max}$  470 nm for MI and 463 nm for the dark state) in comparison to native rhodopsin ( $\lambda_{\max}$  478 nm for MI and 500 nm for the dark state) (34, 35). Fourier transform infrared (FTIR) studies (34, 39) revealed distinct differences between the MI states of 9dm-Rho and native rhodopsin. They also showed, however, that the signaling states MII of the two photoreceptors share a common conformation. In native rhodopsin, transition to MII is accompanied by a deprotonation of the retinal Schiff base and a shift of the visible absorption maximum to 380 nm. In the MII state of 9dm-Rho, the pK<sub>a</sub> of the Schiff base is increased (presumably by a slightly changed position in the protein), and therefore there is only a partial deprotonation of the Schiff base leading to



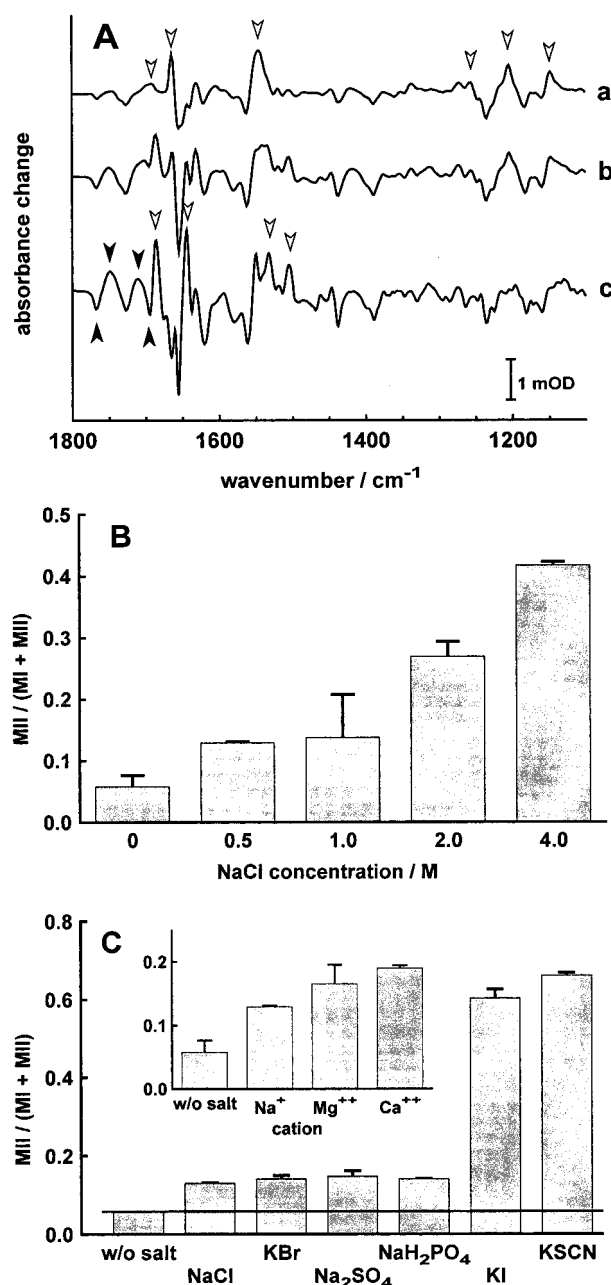


FIGURE 1: Dependence of MII formation on salt concentration and ion specificity in membranes. The MII content of the photoproduct (MI + MII) was determined by FTIR spectroscopy from sandwich samples in membranes buffered with 100 mM MES at pH 4.5 and 1 °C. (A) Representative set of infrared difference spectra recorded without additional salt (a) and with 4 M NaCl (b), as well as from a partially rehydrated film sample with extreme salt concentration (2.5  $\mu$ mol NaCl, corresponding to  $>6$  M). Open arrowheads in traces a and c indicate typical MI and MII difference bands, respectively; black arrowheads indicate bands that were used for evaluation of the MII content. (B) Concentration dependence. The NaCl concentration was varied from 0 to 4 M. (C) Ion specificity. Added salt concentration was 500 mM (250 mM for MgCl<sub>2</sub> and CaCl<sub>2</sub>). The inset shows the dependence of MII formation on the cation of several chloride salts. Addition of 500 mM MES, glycerol, or sucrose showed no increase of the MII content (not shown). The error bars are the SD from duplicate experiments.

the coexistence of two spectrally distinct MII subspecies, MII<sub>380</sub> and MII<sub>470</sub>, absorbing at 380 and 470 nm, respectively (34). Comparison with activation studies of the visual G protein transducin (32) suggests, however, that both species contribute to the active receptor state, which is in full

agreement with the information derived from FTIR spectra. From the FTIR data, it is also evident that the counterion of the dark and MI state of the pigment, Glu<sup>113</sup>, becomes protonated in both MII subspecies (34). In MII<sub>470</sub>, the protonated Schiff base is therefore not stabilized by a charged counterion, but rather by particular dielectric properties of its environment, which are presumably maintained by water molecules accessing the binding pocket.

**Salt Dependence of the MI  $\rightleftharpoons$  MII Equilibrium in Membranes.** We first noticed a salt dependence of the MI  $\rightleftharpoons$  MII equilibrium of 9dm-Rho during FTIR studies on hydrated film samples which were not in agreement with UV-vis results from membrane suspensions or pigment solutions. We could trace back this difference to the high salt concentration ( $\geq 1$  M) due to buffer accumulation in the film samples during the drying and rehydration procedure. To study this effect more systematically, we employed consequently sandwich samples, which have a defined volume and allow a more precise adjustment of both the salt concentration and the pH of the samples (see Experimental Procedures).

Membrane samples (pH 4.5, 1 °C) had in the absence of salts (for simplicity, the term "salt" in this study will not include the buffer substances MES and MOPS for reasons discussed below) only a very low MII content of about 6% of the total photoproduct MI + MII (note that from FTIR spectra we determine the conformational state MII consisting of both sub-species MII<sub>380</sub> and MII<sub>470</sub>, which are distinguished by their absorption maximum in the UV-vis). Addition of NaCl to different concentrations considerably increased the MII content in a concentration-dependent manner, as presented in Figure 1, panels A and B. A similar effect was also observed in attenuated total reflection (ATR) technique, where the membrane film is overlaid by several milliliters of NaCl buffer solution (data not shown) and in sandwich samples with increasing concentration of a phosphate buffer. To determine a putative ion specificity, we tested sodium and potassium salts with different anions (there was no significant specificity for either Na<sup>+</sup> or K<sup>+</sup> when tested as chloride salt). The enhancement was very similar with either 500 mM chloride, phosphate, sulfate, and bromide, which more than doubled the MII content (Figure 1, panel C). A very pronounced effect was seen with both iodide and thiocyanate, which led to a 10-fold increase of the MII content. We observed no increase of the MII content in dependence of the concentration of the buffer substance MES up to 500 mM.

In a second series of measurements (also at pH 4.5), we increased the temperature to 15 °C (data not shown) to increase the MII content of the control (in the absence of salt) to  $\sim 30\%$  and to obtain possibly a more sensitive response of the MI  $\rightleftharpoons$  MII equilibrium already to lower concentrations of salts. However, MII was not significantly increased in the presence of 150 mM NaCl as compared to the control, while 150 mM KI and KSCN increased the MII content considerably to 60–70%. A further increase of the KSCN concentration to 500 mM led at this temperature to a severely distorted difference spectrum reflecting a structural instability and decay of the photoproducts already within the time required for illumination and data acquisition (2 min).

We also observed some specificity for cations (inset in Figure 1, panel C), with Na<sup>+</sup> < Mg<sup>2+</sup> < Ca<sup>2+</sup> in order of

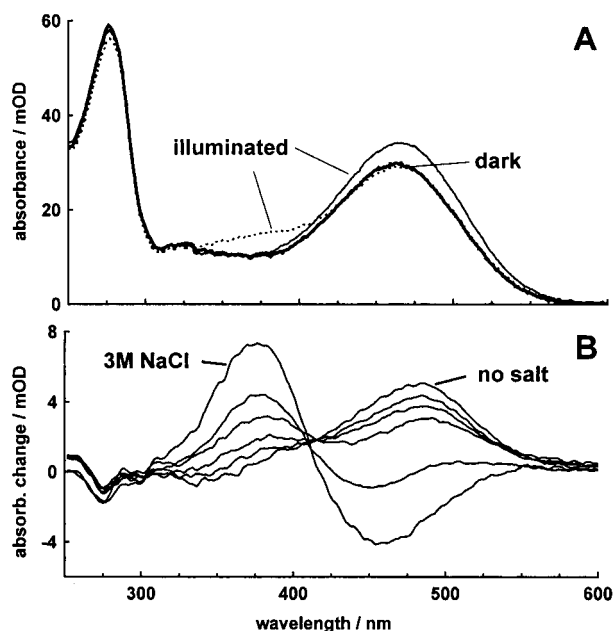


FIGURE 2: NaCl dependence of UV-vis spectra from detergent samples. The spectra were recorded at 10 °C in 20 mM MOPS, pH 7.0, 0.1% DM, in the absence (solid line) and in the presence of 2 M NaCl (dotted line) before and after illumination (A). The difference spectra (illuminated – dark) are shown for samples without, with 250 mM, 500 mM, 1 M, 2 M, and 3 M NaCl (B).

their MII enhancement, tested as chloride salts with a fixed chloride concentration of 500 mM (concentration of divalent cations was therefore half of that of monovalent cations).

Under our experimental conditions, the photoproducts of the pigment were in a steady-state regarding the  $MI \rightleftharpoons MII$  equilibrium. In series of successive spectra recorded after illumination, we detected neither significant changes in this equilibrium over the first few minutes after illumination nor a decay of the photoproducts at 1 °C. Only at higher temperatures, a decay of the photoproducts was observed.

**Salt Dependence of the  $MI \rightleftharpoons MII$  Equilibrium in Detergent Micelles.** FTIR data from solubilized pigments were considerably less reproducible than those from membrane samples. The  $MI \rightleftharpoons MII$  equilibrium is sensitive to both water and detergent content in the samples relative to protein (compare also footnote 2). As the sandwich samples have to be prepared with an excess of buffer to avoid the formation of bubbles in the samples, this leads inevitably to varying water/protein/detergent ratios in the samples due to a hardly controllable loss of detergent and protein with the excess buffer being squeezed out of the sample during preparation. We therefore examined the salt dependence of MII formation in detergent micelles mainly by UV-vis spectroscopy in solutions. In contrast to FTIR spectroscopy, however, we can in the UV-vis not directly determine the total MII content of the photoproduct, but only its  $MI_{380}$  contribution, as well as the total amount of photoproduct,  $MI + MII$ , which is entering our analysis in the photoconversion factor  $\varphi$  (see also Experimental Procedures). In the following, we will therefore analyze  $MI_{380}/(MI + MII)$  for a quantification of active state formation and also discuss salt-dependent shifts in the  $MI_{380} \rightleftharpoons MI_{470}$  protonation equilibrium of MII. As with FTIR membrane samples, the measured photoproduct ratios all correspond to a steady state of the  $MI \rightleftharpoons MII$  equilibrium, and eventual temporal changes

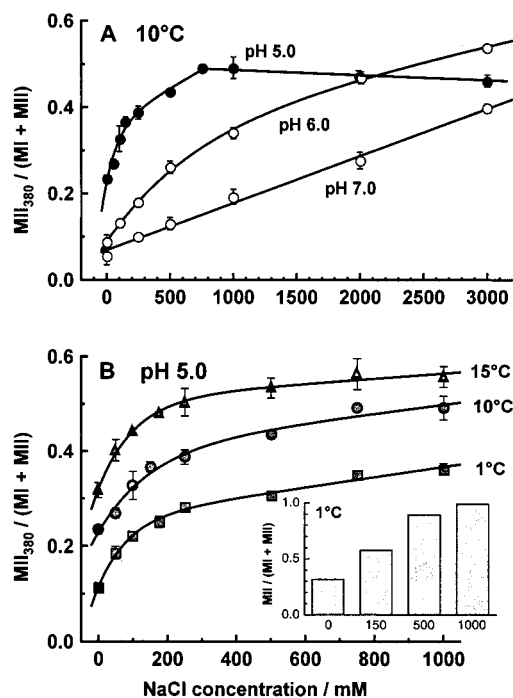


FIGURE 3: Dependence of  $MI_{380}$  formation in detergent micelles on NaCl concentration. The  $MI_{380}$  content of the photoproduct was determined by UV-vis spectroscopy and corrected for the photoconversion  $\varphi$  (see Experimental Procedures). Spectra were recorded from solutions in 0.1% DM buffered by 20 mM MES (MOPS at pH 7.0) (A) at 10 °C and pH 5.0 (black), pH 6.0 (gray) and pH 7.0 (open circles), and (B) at pH 5.0 and 1 °C (squares), 10 °C (circles), and 15 °C (triangles). Illumination conditions were exactly reproduced in all experiments. The inset shows in comparison FTIR results from sandwich samples in detergent measured at 1 °C in 100 mM MES at pH 4.5. Error bars are the SD from 2–6 experiments, solid lines in panel B are fits to the sum of an exponential and a linear function of the concentration.

between successive spectra recorded after illumination, which will be mentioned in the text, always reflected a slow MII decay, which will be discussed in the next section.

In Figure 2, we show a representative set of UV-vis spectra recorded at different NaCl concentrations at pH 7.0 and 10 °C. Evaluation of these spectra (see Experimental Procedures) reveals an almost linear increase of the  $MI_{380}$  content of the photoproducts with NaCl concentration with obviously no saturation even at 3 M salt (Figure 3, panel A). At lower pH, we do observe not only a higher  $MI_{380}$  content of the photoproduct due to the pH dependence of the  $MI \rightleftharpoons MII$  equilibrium but also a more complicated dependence of the  $MI_{380}$  content on NaCl concentration. At pH 6.0, the NaCl dependence of  $MI_{380}$  formation shows a biphasic behavior with a steeper increase at NaCl concentrations below 500 mM. This becomes most pronounced at pH 5.0, where we observe at low concentrations (<200 mM) a steep increase of  $MI_{380}$  (see also Figure 3, panel B, for an enlarged scale). At higher chloride concentrations, there is only a weaker increase, which converts to a slight decrease above 1 M NaCl. The first, steep increase of  $MI_{380}$  at pH 5.0 can certainly be attributed to a salt-dependent shift of the photoproduct equilibrium from MI to MII and a proportional increase of the  $MI_{380}$  subspecies [under low salt conditions, the ratio  $MI_{380}/MII$  was found to be around 0.4 (34)]. At 150 mM NaCl and 10 °C, this equilibrium is already largely shifted to MII, as suggested from FTIR spectra (not shown), and the further, weak  $MI_{380}$  increase

must therefore reflect a salt-dependent shift of the internal  $\text{MII}_{380} \rightleftharpoons \text{MII}_{470}$  protonation equilibrium to the left (unprotonated) side. As Glu<sup>113</sup> is protonated in  $\text{MII}_{470}$  and can therefore not serve as a counterion to the protonated Schiff base in  $\text{MII}_{470}$ , we previously speculated that water molecules in the binding pocket may increase the dielectric constant in the Schiff base environment in MII and thus stabilize the protonated form of the Schiff base (34). Theoretical calculations on retinal Schiff base models emphasize the importance of the dielectric response of the environment on the proton affinity and hence the  $\text{pK}_a$  of the Schiff base (42). Very high salt concentrations, which confer a high osmolarity and therefore a considerably reduced water activity in the buffer, possibly lead to a partial exclusion of water from the retinal binding pocket and a decrease of the dielectric constant. This would in turn negatively affect the mechanism of charge stabilization of the protonated Schiff base and therefore favor its deprotonation. Interestingly, the presence of negatively charged chloride ions in the buffer does not stabilize the protonated form of the Schiff base in 9dm-Rho MII, in contrast to the dark state of the rhodopsin counterion mutants E113Q and E113A. There, a pH- and salt-dependent protonation equilibrium of the Schiff base is formed, in which the protonated form can be stabilized already at low chloride concentrations (43, 44). Obviously, a charge shielding by water is not effective in these mutants, possibly reflecting a tighter protein conformation and a lower water penetration in the dark state in contrast to MII, with its putatively more open structure. In 9dm-Rho MII, we observe at pH 5.0 only above 1 M NaCl a decrease of  $\text{MII}_{380}$ , which, however, rather reflects a slight destabilization of the protein conformation by the concerted action of low pH and high salt concentration, which will be discussed below.

Increasing the temperature not only influences the MII content of the photoproducts in the absence of salts, it also changes the protonation equilibrium  $\text{MII}_{380} \rightleftharpoons \text{MII}_{470}$  in the presence of chloride at pH 5.0 (Figure 3, panel B) by favoring the deprotonated  $\text{MII}_{380}$  subspecies over  $\text{MII}_{470}$ . With 1 M NaCl, the  $\text{MI} \rightleftharpoons \text{MII}$  equilibrium is already at 1 °C largely on the MII side as evident from the FTIR data<sup>2</sup> (see inset in Figure 3, panel B). The increase of the  $\text{MII}_{380}$  yield in the presence of 1 M NaCl from 0.36 at 1 °C to 0.49 at 10 °C and 0.55 at 15 °C therefore reflects a temperature-dependent increase of  $\text{M}_{380}$  at the expense of  $\text{MII}_{470}$  (regarding the data at 15 °C, there may be a slight contribution of hydrolyzed pigment to the 380 nm absorbance at low salt concentrations due to the onset of MII decay). Possibly, the putative salt-dependent partial exclusion of water from the retinal binding pocket is becoming slightly enhanced with increasing temperature. Still, roughly half of the MII photoproduct was present in its protonated form within the range of conditions assayed here.<sup>3</sup> Interestingly, we did not observe an increase of  $\text{MII}_{380}$  in the presence of 100 mM phosphate when increasing the temperature from 10 to 24 °C at pH 4.5 (34), the reason of which being not entirely clear.

<sup>2</sup> Concerning the comparison of data from solutions and FTIR sandwich samples of purified pigment, we found that MII formation is slightly inhibited by increasing detergent concentrations in FTIR samples (Vogel, R., and Siebert, F., unpublished results). As the detergent concentration (and even more the protein concentration) in FTIR samples is higher by at least a factor of 10 as compared to the solution samples, FTIR data rather suggest a lower MII content as compared to data from solutions under otherwise same conditions.

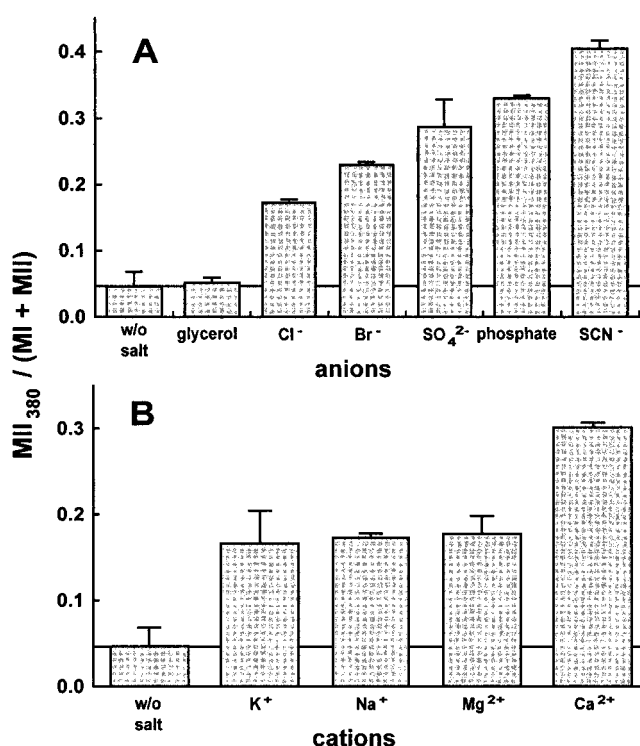


FIGURE 4: Ion specificity of  $\text{MII}_{380}$  formation in detergent micelles. Data acquisition and evaluation were done as in Figure 3.  $\text{MII}_{380}$  content was determined at 10 °C in 20 mM MOPS, pH 7.0. Added salt concentration was 1 M (anion concentration). The anion dependence (A) was determined with sodium salts, the cation dependence with chlorides (B). Glycerol is shown as an example for a nonionic solute. Error bars are the SD from 2–3 experiments.

As will be discussed in the last section of this report, there are presumably two effects contributing to the MII enhancement at pH 5.0 under low salt conditions, namely, a surface pH effect and the Hofmeister effect, while at neutral pH, we expect the Hofmeister effect to be predominant. The very low MII yield at pH 7.0 in the absence of salt also allows us to investigate salt effects at high salt concentrations without being already under saturating MII conditions at least not for moderately chaotropic salts. We therefore examined the ion specificity of the salt-dependent increase of  $\text{MII}_{380}$  formation at 1 M salt at pH 7.0 and 10 °C. As evident from Figure 4, panel A, there is a strong specificity for the anion with  $\text{Cl}^- < \text{Br}^- < \text{SO}_4^{2-} < \text{phosphate} < \text{SCN}^-$  in the order of increasing MII content. Note that with 1 M NaSCN, the  $\text{MII}_{380}$  content is around 0.4, corresponding to a more or less full MII state. The difference between thiocyanate and all other salts may therefore be much more pronounced than suggested by Figure 4, panel A. Iodide led to severe changes

<sup>3</sup> To obtain absolute MII values from UV–vis spectra under conditions with only little MII, as for example in previous transducin activation assays at pH 7.2 and 25 °C (32), we have to extrapolate from conditions where we have full MII and where we can determine the  $\text{MII}_{380}/\text{MII}_{470}$  ratio of MII. At 24 °C and with 100 mM NaCl at pH 5.0,  $\text{MII}_{380}/\text{MII}_{470}$  can be determined to be approximately 1:1 (data not shown). Extrapolating these data, we obtain a second estimate for comparison with the activation assay, in addition to previously calculated MII values based on a constant ratio of only 36:64 as determined in 100 mM phosphate buffer at pH 4.5 and 10 and 24 °C (34). From this second extrapolation, we derive an even more reduced MII content under the conditions of the activation assay, which further corroborates our previous conclusion that this remaining MII content and particularly  $\text{MII}_{470}$  must be fully active in regard to G protein activation.



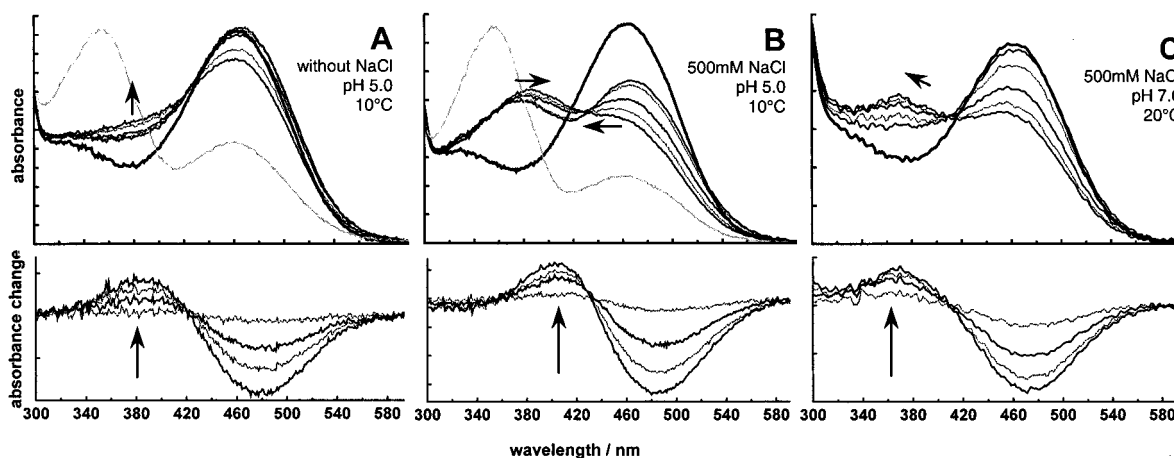


FIGURE 5: Salt dependence of the decay of the photoproducts. 9dm-Rho in detergent solutions (conditions as in Figure 2) was illuminated for 30 s in 20 mM MES (MOPS for pH 7.0), and the decay of the photoproducts was followed spectrophotometrically at 10 °C and pH 5.0 in the absence of salt (A) and with 500 mM NaCl (B), as well as at 20 °C and pH 7.0 with 500 mM NaCl (C). In the upper panels, we show spectra recorded before illumination (solid bold line) and (from top to bottom in the visible region) at  $t = 0$  (solid line), 3 min (dotted), 12 min (solid), 24 min (dotted), and 39 min (solid) after the end of the illumination, as well as after subsequent addition of 30 mM hydroxylamine and warming in the dark to assay photogenerated dark pigment (solid gray line in panels A and B). The spectra in the lower panels are differences of the spectra taken at  $t = 3, 12, 24$ , and 39 min (legend as above) minus the spectrum taken immediately after illumination. Arrows indicate changes of peak positions due to the presence of salt. Tickmarks are 5 mOD.

in the photoproduct spectra and could therefore not be evaluated. The specificity for the cation was assayed with chloride salts with 1 M  $\text{Cl}^-$ . While we found no significant difference between  $\text{K}^+$ ,  $\text{Na}^+$ , and  $\text{Mg}^{2+}$ ,  $\text{Ca}^{2+}$  lead to a considerably increased  $\text{MII}_{380}$  content as compared to the other cations (Figure 4, panel B).

On the other hand, at pH 5.0 and with only 100 mM salt, there is only little specificity for either anion or cation for the moderate salts. The  $\text{MII}_{380}$  yield is at 1 °C between 0.22 and 0.25 for bromide, phosphate, and chloride, the latter as sodium, potassium, calcium, or magnesium salt, as compared to 0.12 without salt (data not shown). Even under these conditions, however, the strong chaotropes thiocyanate and iodide stand out regarding their considerably increased MII yield. FTIR difference spectra from detergent samples revealed that with either 150 mM KI or KSCN the initial photoproduct is already at 1 °C largely MII both at pH 4.5 and 5.5 (data not shown). Among the tested salts, iodide and thiocyanate are therefore most efficient in enhancing MII formation both in membranes and in detergent micelles.

In contrast to the examined salts, we observed with nonionic solutes as glycerol no enhanced MII formation neither with UV-vis (Figure 4, panel A) nor with FTIR spectroscopy. Under certain conditions (e.g., pH 5.0), the MII content in the presence of 100 mM glycerol was even slightly lower than in its absence, suggesting even a stabilization of the MI state. The buffer substances MES and MOPS also led in concentrations up to 500 mM to no increase of the MII content.

**Salts Lead to a Destabilization of the 9dm-Rho Photoproducts.** The effects described above largely affected the steady-state photoproduct equilibria measured within the time scale required for sample illumination and data acquisition (<2 min). In the long term, there are salt-dependent effects on the decay pathways of the photoproducts taking place on a time scale of several minutes up to 1 h, which we will describe in the following.

In Figure 5, the slow decay of the 9dm-Rho photoproducts after illumination is shown. In the absence of salt at 10 °C

and pH 5.0 (Figure 5, panel A), the photoproduct mixture decays slowly to a 380-nm species, as evident from the difference spectra of the decay products (lower panel). This decay product was previously shown to consist of opsin and free retinal by acid denaturation (34). In the presence of 500 mM NaCl, the decay takes a different pathway, and free retinal and opsin are not the predominant decay products as evident from the shifted peak in the difference spectra to >400 nm (Figure 5, panel B, lower panel). Instead, we observe a slow blue shift of the visible absorption peak toward the position of a free protonated Schiff base (at 432 nm in the case of 9-dm retinal as assayed by acid denaturation of 9dm-Rho), indicating a progressive exposure of the Schiff base to the solvent. This can be further confirmed by increasing the pH to 7.0 in the presence of 500 mM NaCl, where we observe a slow decay of the photoproducts to a species with an absorption peak around 365 nm rather than 380 or 430 nm, indicating the deprotonated form of the retinal Schiff base (Figure 5, panel C). Because of the only very slow decay at this pH, the spectra had to be recorded at a higher temperature (20 °C).

In the long term, NaCl therefore destabilizes the photoproducts considerably. With other salts, this effect is even more pronounced. As evident from Figure 6, the velocity of the slow blue shift of the 470 nm photoproduct peak toward the position of the free protonated Schiff base increases with  $\text{NaCl} < \text{KBr} < \text{KSCN}$ . With KSCN, the destabilization of the protein leads additionally to an increase of the Schiff base proton affinity and hence a shift in the  $\text{MII}_{380} \rightleftharpoons \text{MII}_{470}$  protonation equilibrium to the right side. In the presence of 100 mM KI (not shown), the behavior is similar as with KSCN, and the initially red-shifted photoproduct decays to a 430-nm species within 20 min.

The idea of a salt-induced protein destabilization also explains the salt dependence of the critical pH below which we observe a reprotonation of the Schiff base in MII for solubilized pigment. Generally, the  $\text{MII}_{380}$  yield increases with decreasing pH due to an increasing overall MII content and becomes maximal at a certain critical pH. Upon further

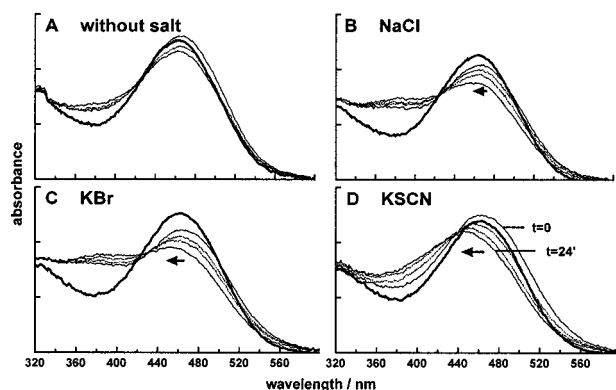


FIGURE 6: Ion specificity of the decay of the photoproducts. 9dm-Rho in detergent micelles was illuminated for 30 s at 10 °C in 20 mM MES, pH 5.0, and the decay of the photoproducts was followed spectrophotometrically in the absence of additional salt (A) and in the presence of 100 mM NaCl (B), KBr (C), or KSCN (D). The spectra were recorded before illumination (solid bold line) and (from top to bottom in the visible region) at  $t = 0$  (solid line), 6 min (dotted), 12 min (dotted), and 24 min (solid) after the end of the illumination. The arrows indicate the progressive blue shift of the visible photoproduct peak with time. Tickmarks are 10 mOD.

lowering the pH,  $\text{MII}_{380} \rightleftharpoons \text{MII}_{470}$  decreases due to a shift in the  $\text{MII}_{380} \rightleftharpoons \text{MII}_{470}$  protonation equilibrium to the right side (34). In the absence of a Hofmeister salt (e.g., in 10 or 100 mM MES) or in 10 mM phosphate buffer, this critical pH was found to be around 4.0 and to increase to 4.5 in 100 mM phosphate buffer (data not shown). At pH 5.0, 1 M NaCl are required to force reprotonation of the Schiff base by presumably the same mechanism (Figure 3, panel A). Because of the pronounced dependence on salt concentration, these results may reflect a pH-induced change of the photoproduct conformation leading to a slight increase of the intrinsic proton affinity of the Schiff base. Consequently, destabilizing effects of low pH and salt may add up and lead to a higher pH sensitivity in the presence of salt than in its absence. In Figure 6, panel D, we see a similar shift of  $\text{MII}_{380} \rightleftharpoons \text{MII}_{470}$  to the right side in the presence of 100 mM KSCN immediately after illumination, which is followed by an overall instability of the photoproducts on the much longer time scale of 10–20 min. This may suggest a sequential mechanism of destabilization, with changes that affect only a limited region of the protein preceding those involving the entire protein. In summary, the shift of the  $\text{MII}_{380} \rightleftharpoons \text{MII}_{470}$  equilibrium to the right side likely reflects pH- and salt-induced slight structural changes of the MII state and should not be confused with the general, salt-dependent shift to the left side described above, which is presumably due to a decreased water activity and a less efficient shielding and stabilization of a protonated Schiff base in the protein interior.

We therefore can distinguish between three different effects of salts on the 9dm-Rho photoproducts: (i) an effect on the conformation of the intact protein, shifting the  $\text{MI} \rightleftharpoons \text{MII}$  equilibrium, (ii) a (slower) destabilization of the entire protein, and (iii) a presumably indirect influence on the protonation equilibrium of the MII subspecies,  $\text{MII}_{380} \rightleftharpoons \text{MII}_{470}$ , by a lowered water activity, which does not affect the integrity of the protein. While the latter effect is restricted on particular properties of the protein under investigation here, the other two are presumably rather general than specific. It will therefore be rewarding to discuss the

underlying mechanisms more in detail in the following section.

*How Can Salts Interact with the Protein in the Framework of the Hofmeister Effect?* All salts that were examined here, including NaCl, clearly show a chaotropic behavior by destabilizing the photoproducts of 9dm-Rho. Cosmotropic effects, which would arise from a salt-dependent increase of the surface tension of the aqueous phase, lead to an increase of the free energy required for forming a molecular size cavity in the aqueous phase, and favor a salting-out of hydrophobic groups, are not detectable. We can therefore conclude that interactions with hydrophobic groups probably play only a minor role in our system. This is different for many soluble proteins, where we can well distinguish between cosmotropic and chaotropic salts (and where therefore both modes of action contribute to the observed effects), and where, for example, NaCl is rather a cosmotrope (20). Soluble proteins are mainly stabilized by the hydrophobic collapse of buried nonpolar residues such that a salting-out of hydrophobic residues leads to a stabilization of the protein structure. For GPCRs as seven-helix transmembrane proteins and possibly also for other membrane proteins, the situation is different. Helix–helix stabilization is believed to be not driven by a hydrophobic collapse (45, 45), especially as there are a number of polar residues in the protein transmembrane core of GPCRs. Considering the hydrophobicity of the embedding lipid phase, we can rather speak of the contrary, that is, of a hydrophilic collapse (46), which is also supported by recent studies on engineered hydrophobic peptides with one hydrophilic asparagine (47, 48). In model systems of transmembrane helix dimers lacking polar groups (glycophorin A), association of helix pairs rather depends on the existence of preformed complementary interfaces, which involves a minimization of steric clashes between juxtaposed side chains of helix pairs, thus maintaining favorable van der Waals contacts, as well as only little freezing out of side chain rotamers during the association process (49). This tight interaction between helices is also reflected in the significantly higher helix packing ratio of integral membrane proteins as compared to soluble proteins (45). In summary, the absence of pronounced cosmotropic effects of salts in our study is therefore not as astonishing.

The transition from rhodopsin MI to MII is known to involve major structural changes, mainly acting on the cytoplasmic side of the protein. These changes involve a relative rigid-body movement of helix 3 and 6 (50–52). Cross-linking of the cytoplasmic termini of these helices by either the introduction of metal ion binding sites or disulfide bridges abolishes this motion and was shown to prevent transducin activation (51, 53). Site-directed spin-labeling of residues on the solvent-exposed cytoplasmic loops revealed changes in the structure of the second and fourth loop upon transition from the dark state to MII but not from the dark state to MI (54). Similar changes were found by FTIR spectroscopy of partially protease-digested rhodopsin (55). The latter results indicated that part of the structural changes taking place during the transition from the dark state to MII can be ascribed to changes in the protease-accessible cytoplasmic loop regions and that the accessibility for proteases is higher in MII than in the dark state. Finally, the accessibility and binding of a specific antibody to an epitope



comprising the cytoplasmic half of helix 7 was also found to correlate with formation of MII (56).

We therefore propose that the chaotropic salts act on the  $MI \rightleftharpoons MII$  equilibrium by an increased solvation of the (presumably cytoplasmic) loop domains due to a salting-in of the peptide backbone. As the cytoplasmic domain is likely to be more disordered in MII as compared to MI (or the dark state), this interaction leads to a corresponding shift in the photoproduct equilibrium to MII. A salting-in of the peptide backbone may also weaken other stabilizing conformational constraints located at the cytoplasmic helix termini that otherwise keep the receptor in its inactive conformation. Importantly, this salt-dependent interaction does not necessarily affect the integrity of the photoproducts, as verified by both UV-vis and FTIR spectra at moderate concentrations of moderately chaotropic salts. Only at high salt concentrations, in the presence of strong chaotropes as KI or KSCN, or in the long-term decay processes, we observe structural changes between normal (i.e., not salt-induced) MII and salt-enhanced MII. On this later stage, the salting-in of the solvent-exposed domains presumably extends deeper into the core of the transmembrane helix bundle. Helix-helix interactions will then be weakened and the structural stability of the protein will be lost. Somewhere on the path to this overall destabilization of the protein, the retinal Schiff base in the core of the protein becomes exposed to the solvent, thereby leading to the observed shift of the UV-vis absorption peaks toward the same position as in a denatured protein. A similar sequential mechanism is also observed in the SDS-induced destabilization of another membrane protein, diacylglycerol kinase, involving first mainly cytoplasmic protein domains and only in a second phase also the more stable transmembrane helical domain (57). In that protein, as well as in other membrane proteins as, for example, bacteriorhodopsin (58), most of the native helical content is retained during unfolding.

A correlation between enhanced activity and structural instability is also observed in constitutively active mutants of other transmembrane receptor proteins. In the  $\beta_2$  adrenergic receptor, mutations that favor the active receptor state (both in the absence or presence of an agonist) were shown to increase the flexibility of the receptor due to disruption of stabilizing conformational constraints, and to confer, in the long term, also structural instability to the protein (59, 60). Possibly similar arguments apply also to the histamine  $H_2$  receptor (61).

*The MII Enhancement Cannot Be Explained by Osmolarity or a Surface pH Effect alone.* It was shown recently that the MI to MII transition of rhodopsin in membranes is accompanied by a release of a number of water molecules (62), which are presumably peripherally bound to the ordered solvent-exposed domains in MI. The presence of an osmotically active cosolute will therefore shift the  $MI \rightleftharpoons MII$  equilibrium to the MII side. To test, whether the MII enhancement observed in our experiments can be primarily due to the increased osmolarity of the buffer in the presence of salt, we measured the influence of nonionic or zwitterionic cosolutes on the  $MI \rightleftharpoons MII$  equilibrium. In FTIR experiments with 500 mM glycerol or sucrose at 1 °C and pH 4.5, we found no significant increase of the MII content as compared to the control. Similarly, neither UV-vis nor FTIR results were affected significantly by changing the concentration of

the buffer substance MES from 20 to 100 mM or from 100 to 500 mM, respectively. Presumably, MES may be active as an osmotic cosolute but not as a Hofmeister salt. This lack of evidence for an osmotically driven MII formation in our experiments does not necessarily contradict the above-mentioned experiments of Mitchell and Litman (62), as their effect is considerably smaller as compared to the salt effect described here. An increase of the buffer osmolality by 0.6 (which is the approximate osmolality of 500 mM glycerol) increased the logarithm of  $K = MII/MI$  by approximately 0.2 in their experiments. Under our FTIR conditions (pH 4.5, 1 °C), this only corresponds to a very slight increase of the MII yield from 0.06 of the control to 0.07, which would be undetectable. DeLange et al. also found for nonionic or zwitterionic cosolutes as betaine no significant increase of MII of rhodopsin in membranes (10). We found for glycerol no effect or even a slight decrease of the  $MI_{380}$  content in detergent micelles as compared to the control. This suggests, that the MII enhancing effect of mere osmolarity may be even overcompensated under these conditions by a cosmotropic or stabilizing effect of glycerol, which is described elsewhere (13).

A salt-induced shift of the photoproduct equilibrium of rhodopsin was observed before by DeLange et al. (10) with similar results as here, yet only for pigment in disk membranes. They found for KCl both a concentration-dependent increase of the apparent  $pK_a$  of the pH-dependent  $MI \rightleftharpoons MII$  equilibrium (and thus an increased MII production) and an increase of the apparent rate constant of the transition, of which the latter was already described before in detergent (9). The MII enhancement was tested for 1 M salt solutions in membranes with a salt specificity of  $NaCl < KCl < CaCl_2$  (only 500 mM)  $\approx$   $KBr < KI < KSCN$  in increasing order, which is very similar to the ion specificity observed in our experiments with 9dm-Rho. The decay rate of MII was reported to be salt independent. DeLange et al. tentatively interpreted their data as a result of a surface pH effect. From the amino acid sequence, they deduced a positive net charge for the cytoplasmic side of the disk membranes, which would increase the local pH at the surface of the membranes due to electrostatic repulsion of protons. Increasing salt concentrations may shield surface charges and thus lead to an adjustment (in this case lowering) of the local pH to the bulk pH. A lowered surface pH would in turn force protonation of Glu<sup>134</sup> at the cytoplasmic end of helix 3, which is believed to govern the pH-dependent transition from MI to MII (63, 64). The ion specificity was assigned to gradually differing lipophilic properties of the anions, allowing them to affect also buried pH-sensitive residues regulating the MI to MII transition, particularly at very high salt concentrations. It was shown later that a surface pH effect on the  $MI \rightleftharpoons MII$  equilibrium can indeed be observed and that it quantitatively obeys the Gouy-Chapman equation (11). Yet, this effect was actually in the opposite direction than proposed by DeLange et al., as the asymmetric distribution of lipids, namely, of phosphatidylserines in the disk membranes, also contributes to the surface charge of disk membranes. This leads to a negative net charge on the cytoplasmic surface (65) and thus to a decrease of the surface pH as compared to the bulk. Increasing the salt concentration should, therefore, at constant bulk pH, increase the surface pH and lower the extent of MII formation. This salt effect due to surface

charge shielding saturates in membranes already around 100 mM salt (11) and is presumably the reason why we observe in our experiments on membrane samples no effect of NaCl on the MII yield at low (150 mM) concentrations, as both effects (surface pH and Hofmeister effect) may be balanced out. Only the strong destabilizers as KI and KSCN show at this concentration already a considerable MII enhancement.

In micelles of nonionic detergent molecules as DM, the negative charge contribution of phosphatidylserines is absent, and we have therefore a net positive charge at rhodopsin's cytoplasmic surface domain at neutral to acidic pH (cf. ref 65). Under these conditions, salts can actually lower the surface pH as compared to the bulk and thus favor MII formation. An analytical approach to determine the extent of such a contribution is difficult, as the Gouy–Chapman framework requires a smeared charge distribution on a more or less planar surface. In contrast to rhodopsin in disk membranes, rhodopsin in a detergent micelle does certainly not fulfill these requirements. To obtain an estimate of such a contribution and to distinguish it from the Hofmeister effect, we can decrease the titratable surface charges on the cytoplasmic protein domain (from  $\sim +7$  at pH 5.0  $\sim +4$  at pH 7.0 employing model  $pK_a$ 's from ref 65 to obtain a rough estimate) simply by increasing the buffer pH.

Indeed, the dependence of the MII<sub>380</sub> yield on NaCl concentration in detergent presented in Figure 3 is at pH 7.0 no longer biphasic but linear, suggesting that the underlying mechanism does not saturate at higher salt concentrations. This excludes a large contribution of a surface pH effect at this pH, as salt effects on surface charges should saturate already at low to intermediate salt concentrations (11). The Hofmeister effect, on the other hand, does not saturate even at high salt concentrations (15, 18), which agrees with our experiments, where we observe saturation neither in detergent nor in membranes (Figure 1, panel B). At lower pH, there is likely a contribution from the surface pH effect to the observed salt-dependent MII<sub>380</sub> increase in detergent. This becomes evident from the ion specificity, which shows at pH 7.0 significant differences also between the moderate salts (in the sense of the Hofmeister effect, Figure 4) but is vanishing at pH 5.0 (described in the text). This observation can be explained by the contribution of the surface pH effect, which is dependent on ionic strength only and not on the specific ion and which may therefore disguise any ion specificity due to the Hofmeister effect for the weak chaotropes. Under these conditions, only the strong chaotropes thiocyanate and iodide lead to an outstandingly higher MII yield, reflecting the pronounced ion specificity of the Hofmeister effect.

A further interesting point is the considerable MII enhancement in the presence of sodium sulfate in detergent (Figure 4, panel A) but also in membranes (Figure 1, panel C), which is not in line with the Hofmeister series, where sodium sulfate is only a very weak chaotrope. Possibly, ionic strength, which is considerably higher for equimolar concentrations of divalent as compared to monovalent salts, also contributes to the MII enhancement by screening of the Coulombic interaction of charged residues in the protein. As this effect persists at relatively high ionic strength, this/these residue(s) should only be partially accessible to the solvent. Recently, the influence of salt on the stabilizing properties of salt bridges and its correlation with the solvent acces-

sibility of the respective sites was shown for human lysozyme (66). Such a mechanism, depending on ionic strength only, would in our study apply to all salts and contribute in addition to the highly ion-selective Hofmeister effect and is currently being investigated.

In summary, our results can be consistently interpreted in the framework of the Hofmeister effect and be specifically explained by a salt-dependent increased solvation of the protein and a weakening of conformational constraints. The described effects of salts on the conformational equilibria and the stability of 9-demethyl rhodopsin do not depend on specific properties of this protein as a visual pigment. As rhodopsin is a prototypical G protein-coupled receptor, these results very likely apply to the whole family of heptahelical transmembrane receptors. We therefore expect a general dependence of the equilibria between inactive and active receptor conformations (either agonist-bound or free) on the presence of salts. The proposed mechanism putatively involves first an increased solvation and disordering of solvent-exposed protein domains. The resulting structural changes in these domains may then lead to a rearrangement of the  $\alpha$ -helical transmembrane domain. This may leave secondary structural elements intact but changes the tertiary structure and thus the conformation of the protein. Such a sequential mechanism may be a general aspect of the action of salts on membrane proteins. In addition, these general salt effects on proteins may be of considerable importance, for example, for infrared spectroscopy, where sample preparation frequently involves drying and rehydration of protein solutions and thus a usually unintended accumulation of salts.

## ACKNOWLEDGMENT

We thank Bettina Maier for her excellent technical assistance during protein preparation.

## REFERENCES

1. Baldwin, J. M. (1993) *EMBO J.* 12, 1693–1703.
2. Hofmann, K. P. (1986) *Photobiochem. Photobiophys.* 13, 309–327.
3. Gether, U., and Kobilka, B. K. (1998) *J. Biol. Chem.* 273, 17979–17982.
4. Strader, C. D., Fong, T. M., Tota, M. R., and Underwood, D. (1994) *Annu. Rev. Biochem.* 63, 101–132.
5. Sakmar, T. P. (1998) *Prog. Nucleic Acid Res. Mol. Biol.* 50, 1–34.
6. Parkes, J. H., and Liebman, P. A. (1984) *Biochemistry* 23, 5054–5061.
7. Lamola, A. A., Yamane, T., and Zipp, A. (1974) *Biochemistry* 13, 738–745.
8. Baldwin, P. A., and Hubbell, W. L. (1985) *Biochemistry* 24, 2624–2632.
9. Arnis, S., and Hofmann, K. P. (1993) *Proc. Natl. Acad. Sci. U.S.A.* 90, 7849–7853.
10. Delange, F., Merckx, M., Bovee-Geurts, P. H., Pistorius, A. M., and DeGrip, W. J. (1997) *Eur. J. Biochem.* 243, 174–180.
11. Gibson, S. K., Parkes, J. H., and Liebman, P. A. (1999) *Biochemistry* 38, 11103–11114.
12. Hofmeister, F. (1888) *Arch. Exp. Pathol. Pharmacol.* 24, 247–260.
13. Cacace, M. G., Landau, E. M., and Ramsden, J. J. (1997) *Q. Rev. Biophys.* 30, 241–277.
14. Collins, K. D., and Washabaugh, M. W. (1985) *Q. Rev. Biophys.* 18, 323–422.
15. Baldwin, R. L. (1996) *Biophys. J.* 71, 2056–2063.

16. Melander, W., and Horvath, C. (1977) *Arch. Biochem. Biophys.* 183, 200–215.
17. Nandi, P. K., and Robinson, D. R. (1972) *J. Am. Chem. Soc.* 94, 1308–1315.
18. Nandi, P. K., and Robinson, D. R. (1972) *J. Am. Chem. Soc.* 94, 1299–1308.
19. Breslow, R., and Guo, T. (1990) *Proc. Natl. Acad. Sci. U.S.A.* 87, 167–169.
20. Yamasaki, M., Yano, H., and Aoki, K. (1991) *Int. J. Biol. Macromol.* 13, 322–328.
21. Damodaran, S. (1989) *Int. J. Biol. Macromol.* 11, 2–8.
22. Yun, C. H., Song, M., Ahn, T., and Kim, H. (1996) *J. Biol. Chem.* 271, 31312–31316.
23. Dér, A., and Ramsden, J. J. (1998) *Naturwissenschaften* 85, 353–355.
24. Ebel, C., Faou, P., Kernel, B., and Zaccai, G. (1999) *Biochemistry* 38, 9039–9047.
25. Jensen, W. A., Armstrong, J. M., De Giorgio, J., and Hearn, M. T. (1996) *Biochim. Biophys. Acta* 1296, 23–34.
26. Jensen, W. A., Armstrong, J. M., De Giorgio, J., and Hearn, M. T. (1995) *Biochemistry* 34, 472–480.
27. Schrammel, A., Gorren, A. C., Stuehr, D. J., Schmidt, K., and Mayer, B. (1998) *Biochim. Biophys. Acta* 1387, 257–263.
28. von Hippel, P. H., and Wong, K. Y. (1962) *Biochemistry* 1, 664–674.
29. Lusitani, D., Menhart, N., Keiderling, T. A., and Fung, L. W. (1998) *Biochemistry* 37, 16546–16554.
30. Corson, D. W., Cornwall, M. C., MacNichol, E. F., Tsang, S., Derguini, F., Crouch, R. K., and Nakanishi, K. (1994) *Proc. Natl. Acad. Sci. U.S.A.* 91, 6958–6962.
31. Morrison, D. F., Ting, T. D., Vallury, V., Ho, Y. K., Crouch, R. K., Corson, D. W., Mangini, N. J., and Pepperberg, D. R. (1995) *J. Biol. Chem.* 270, 6718–6721.
32. Han, M., Groesbeck, M., Smith, S. O., and Sakmar, T. P. (1998) *Biochemistry* 37, 538–545.
33. Shieh, T., Han, M., Sakmar, T. P., and Smith, S. O. (1997) *J. Mol. Biol.* 269, 373–384.
34. Vogel, R., Fan, G. B., Sheves, M., and Siebert, F. (2000) *Biochemistry* 39, 8895–8908.
35. Meyer, C. K., Böhme, M., Ockenfels, A., Gärtner, W., Hofmann, K. P., and Ernst, O. P. (2000) *J. Biol. Chem.* 275, 19713–19718.
36. Gether, U., Lin, S., Ghanouni, P., Ballesteros, J. A., Weinstein, H., and Kobilka, B. K. (1997) *EMBO J.* 16, 6737–6747.
37. Rasmussen, S. G., Jensen, A. D., Liapakis, G., Ghanouni, P., Javitch, J. A., and Gether, U. (1999) *Mol. Pharmacol.* 56, 175–184.
38. Kahlert, M., König, B., and Hofmann, K. P. (1990) *J. Biol. Chem.* 265, 18928–18932.
39. Ganter, U. M., Schmid, E. D., Perez-Sala, D., Rando, R. R., and Siebert, F. (1989) *Biochemistry* 28, 5954–5962.
40. DeGrip, W. J. (1982) *Methods Enzymol.* 81, 197–207.
41. Fahmy, K., Jäger, F., Beck, M., Zvyaga, T. A., Sakmar, T. P., and Siebert, F. (1993) *Proc. Natl. Acad. Sci. U.S.A.* 90, 10206–10210.
42. Tajkhorshid, E., and Suhai, S. (1999) *Chem. Phys. Lett.* 299, 457–464.
43. Nathans, J. (1990) *Biochemistry* 29, 9746–9752.
44. Sakmar, T. P., Franke, R. R., and Khorana, H. G. (1991) *Proc. Natl. Acad. Sci. U.S.A.* 88, 3079–3083.
45. Eilers, M., Shekar, S. C., Shieh, T., Smith, S. O., and Fleming, P. J. (2000) *Proc. Natl. Acad. Sci. U.S.A.* 97, 5796–5801.
46. Engelman, D. M., and Zaccai, G. (1980) *Proc. Natl. Acad. Sci. U.S.A.* 77, 5894–5898.
47. Choma, C., Gratkowski, H., Lear, J. D., and DeGrado, W. F. (2000) *Nat. Struct. Biol.* 7, 161–166.
48. Zhou, F. X., Cocco, M. J., Russ, W. P., Brunger, A. T., and Engelman, D. M. (2000) *Nat. Struct. Biol.* 7, 154–160.
49. MacKenzie, K. R., and Engelman, D. M. (1998) *Proc. Natl. Acad. Sci. U.S.A.* 95, 3583–3590.
50. Farahbakhsh, Z. T., Hideg, K., and Hubbell, W. L. (1993) *Science* 262, 1416–1419.
51. Farrens, D. L., Altenbach, C., Yang, K., Hubbell, W. L., and Khorana, H. G. (1996) *Science* 274, 768–770.
52. Dunham, T. D., and Farrens, D. L. (1999) *J. Biol. Chem.* 274, 1683–1690.
53. Sheikh, S. P., Zvyaga, T. A., Lichtarge, O., Sakmar, T. P., and Bourne, H. R. (1996) *Nature* 383, 347–350.
54. Resek, J. F., Farahbakhsh, Z. T., Hubbell, W. L., and Khorana, H. G. (1993) *Biochemistry* 32, 12025–12032.
55. Ganter, U. M., Charitopoulos, T., Virmaux, N., and Siebert, F. (1992) *Photochem. Photobiol.* 56, 57–62.
56. Abdulaev, N. G., and Ridge, K. D. (1998) *Proc. Natl. Acad. Sci. U.S.A.* 95, 12854–12859.
57. Lau, F. W., and Bowie, J. U. (1997) *Biochemistry* 36, 5884–5892.
58. Brouillette, C. G., Muccio, D. D., and Finney, T. K. (1987) *Biochemistry* 26, 7431–7438.
59. Gether, U., Ballesteros, J. A., Seifert, R., Sanders-Bush, E., Weinstein, H., and Kobilka, B. K. (1997) *J. Biol. Chem.* 272, 2587–2590.
60. Samama, P., Bond, R. A., Rockman, H. A., Milano, C. A., and Lefkowitz, R. J. (1997) *Proc. Natl. Acad. Sci. U.S.A.* 94, 137–141.
61. Alewijnse, A. E., Timmerman, H., Jacobs, E. H., Smit, M. J., Roovers, E., Cotecchia, S., and Leurs, R. (2000) *Mol. Pharmacol.* 57, 890–898.
62. Mitchell, D. C., and Litman, B. J. (1999) *Biochemistry* 38, 7617–7623.
63. Fahmy, K., and Sakmar, T. P. (1993) *Biochemistry* 32, 7229–7236.
64. Fahmy, K., Sakmar, T. P., and Siebert, F. (2000) *Biochemistry* 39, 10607–10612.
65. Tsui, F. C., Sundberg, S. A., and Hubbell, W. L. (1990) *Biophys. J.* 57, 85–97.
66. Takano, K., Tsuchimori, K., Yamagata, Y., and Yutani, K. (2000) *Biochemistry* 39, 12375–12381.

BI001855R